

Characterization and stability measurement of deployed multicore fibers for quantum applications

Davide Bacco^{1,*}, Nicola Biagi^{2,3}, Ilaria Vagniluca^{2,4}, Tetsuya Hayashi⁵, Antonio Mecozzi^{6,7}, Cristian Antonelli^{6,7}, Leif K. Oxenløwe¹, and Alessandro Zavatta^{2,3}

¹*CoE SPOC, DTU Fotonik, Technical University of Denmark, 2800 Kgs. Lyngby, DK*

²*Istituto Nazionale di Ottica (CNR-INO), Largo E. Fermi 6, 50125 Florence, IT*

³*LENS and Department of Physics and Astronomy, University of Florence, 50019 Sesto Fiorentino, IT*

⁴*Department of Physics "Ettore Pancini", University of Naples "Federico II", Via Cinthia 21, 80126 Naples, IT*

⁵*Optical Communications Laboratory, Sumitomo Electric Industries, Ltd., 244-8588 Yokohama, JP*

⁶*Department of Physical and Chemical Sciences, University of L'Aquila, L'Aquila, IT*

⁷*National Laboratory of Advanced Optical Fibers for Photonics (FIBERS), CNIT, L'Aquila, Italy*

**dabac@fotonik.dtu.dk*

Abstract

Multicore fibers are expected to be a game-changer in the coming decades thanks to their intrinsic properties, allowing a larger transmission bandwidth and a lower footprint in optical communications. In addition, multicore fibers have recently been explored for quantum communication, attesting their uniqueness in transporting high-dimensional quantum states. However, investigations and experiments reported in literature have been carried out in research laboratories, typically making use of short fiber links in controlled environments. Thus, the possibility of using long distance multicore fibers for quantum applications is still to be proven. We here characterize for the first time, in terms of phase stability, multiple strands of a 4-core multicore fiber installed underground in the city of L'Aquila, with an overall fiber length up to about 25 km. In this preliminary study, we investigate the possibility of using such an infrastructure to implement quantum-enhanced schemes, such as high-dimensional quantum key distribution, quantum-based environmental sensors, and more in general quantum communication protocols.

Introduction

Multicore fibers (MCFs), i.e., optical fibers with multiple cores within the same cladding, are expected to be a game-changer in the next generation of telecommunication infrastructures [1–4]. In fact, multicore fibers present multiple advantages over standard single-mode fibers, while maintaining, at the same time, a similar performance in terms of optical loss [5, 6]. Specifically, multicore fibers constitute a promising candidate for the implementation of space-division multiplexed transmission, and their standardization is taken into considered [7]. They present a lower footprint, which is of high importance in the deployment process, e.g., in telecom data-centers where the space is limited, and they allow the use of a single amplifier for all the cores, reducing the number of resources [8]. Furthermore, multicore fibers represent a perfect match with photonic integrated circuits for multiple-input-multiple-output applications, and are expected to be widely adopted in long-haul undersea connections [9]. Recently, multicore fibers have also been tested for quantum communication [10–17]. Thanks to their properties of low loss and small crosstalk between the different

cores, these fibers, which are referred to as uncoupled-core MCFs, have been used for co-propagating quantum and classical signals in different cores [10], or in the same core [11, 12], and also for transmitting high-dimensional quantum states [13–17]. High-dimensional quantum states, thanks to their intrinsic properties, allow for a higher information capacity (useful in the case of a limited photon budget or in the regime of saturating single-photon detectors) and also exhibit higher robustness to the noise affecting the quantum communication (which is critical in real-world applications) [18]. However, the transmission of high-dimensional quantum states over multicore fibers requires phase stability between the different cores, since the quantum states are encoded in coherent superpositions of the cores of the fiber. In fact, although the improved phase stability of a single multicore fiber, compared to a bundle of single-core fibers, was already demonstrated over 2 km of a 7-core uncoupled fiber (in laboratory environment), the phase stability of longer deployed MCFs was never tested so far [17, 19, 20]. In this work, we study the phase stability of a 4-core uncoupled multicore fiber with 25.16 km of length, deployed in the city of L'Aquila [4]. Furthermore, we propose and demon-

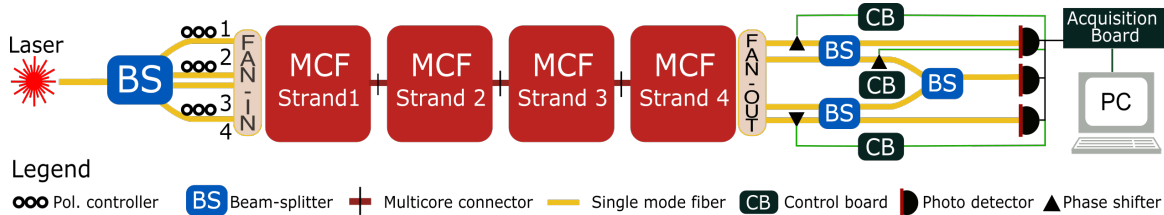


Figure 1: Experimental setup. A continuous wave laser at 1550 nm is equally divided into four paths through a 1x4 beam splitter (BS). The four single-mode fibers are then individually connected to the fan-in input of the multicore fiber. Thanks to the reconfigurability of the optical system, it is possible to set the number of subsequent MCF strands to be tested in the experiment (each strand is approximately 6.29 km of length). To connect the strands to each other, a multicore fiber connector is used. After propagation through the MCF, a fan-out device is used to divide the cores into four different single-mode fibers, that are finally combined with each other by three 2x2 beam splitters. By using three automatic control boards, each driving a phase shifter, based on the measurement output of the three detectors, we can monitor and individually control the relative phase of each core.

strate a scalable fully-automatic stabilization method which is potentially useful in transporting and manipulating the high-dimensional quantum states over a multicore fiber.

Experimental setup

In our experiment we have used an optical test-bed infrastructure built in 2019 in the city of L’Aquila [4]. A single jelly-filled loose-tube cable, with an outer diameter of 6 mm and a total length of 6.29 km, has been deployed in a multi-service underground tunnel with both ends accessible from the same location. The cable accommodates three different kinds of multicore fibers for a total of 18 strands: twelve are randomly-coupled 4-cores MCFs (RC-4CF), four are uncoupled 4-cores MCFs (UC-4CF) and two are uncoupled 8-cores MCFs (UC-8CF). The first two kinds (RC-4CF and UC-4CF) are optimized for the C-band window (1550 nm), while the latter (UC-8CF) is optimized for the O-band window (1310 nm). All the cores in each strand are accessible via an optical patch panel. More details are reported in the work by T. Hayashi and co-authors [4]. In our experiment, we focused on the UC-4CF strands, which to date have been characterized only with respect to inter-core crosstalk [4] and time skew [21, 22]. All the UC-4CF strands are terminated by spliced SC-connectorized MCF pigtails on both ends. This allows to concatenate multiple strands, up to a total MCF length of 25.16 km, or to access each core individually by connecting the strand to a fan-in fan-out device, that splits the four cores into four different single-mode fibers.

In order to adopt the MCF for quantum applications, an efficient stabilization of the relative phase between all the different cores is required. Figure 1 shows the interferometric scheme we have implemented to test the phase stability of the UC-4CF. The output of a continuous wave laser emitting at 1550 nm has been injected into the common port of a 1x4 fiber

beam-splitter (BS). After the beam-splitter, we have inserted 3 fiber-based polarization controllers to correctly aligned the polarization inside the different cores of the fiber. The output ports have been connected to the four cores of a UC-4CF strand, through the fan-in device. The end of this strand can be connected directly to the last part of the interferometric setup, by using the fan-out kit, or to the input of another UC-4CF strand. In this way, we can adjust the overall interferometer length from 6.29 km to 25.16 km, by steps of 6.29 km. The four cores of the last connected strand, after the fan-out kit, have been injected into the input ports of two 2x2 BSs. Thus, two independent 2-path interferometers between cores 1 & 2 and cores 3 & 4, respectively, have been realized. By monitoring one output port of each interferometer, we can measure the relative phase fluctuations between cores 1 & 2 and cores 3 & 4, as shown in Figure 1. Moreover, by combining the remaining output ports of the 2-path interferometers via a third 2x2 BS, we can access the relative phases between all of the cores. The three interferometer outputs were monitored with p-i-n photodiodes, resulting in three electrical signals that were collected with a *National Instruments* Data Acquisition Board (NI Daq) , connected to a computer (PC).

In order to fully and individually control the relative phases between the four uncoupled cores, a Phase Lock Loop (PLL) has been integrated in each interferometer. The main component of each PLL is the control board (CB) composed by an ADuC7020 microcontroller unit (MCU), produced by Analog Devices. This device incorporates a 5-channels 12-bit analog-to-digital converter (ADC) and a 4-channels 12-bit digital-to-analog converter (DAC). Thanks to the high resolution of the analog channels, and to the MCU clockrate of 41.78 MHz, this microcontroller is suitable to implement a digital proportional-integral-derivative controller (PID), able to efficiently stabilize the MCF interferometers. In order to maximize the computa-

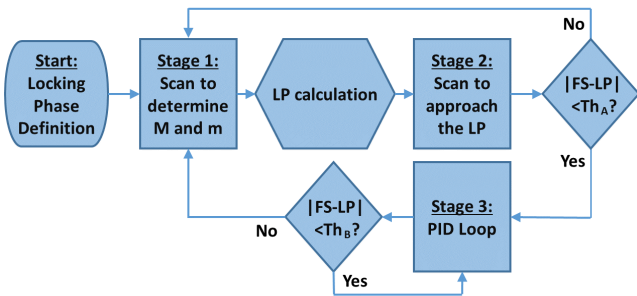


Figure 2: Flow chart of the PID controller. This algorithm is used for controlling each phase-shifter in the three different interferometers.

tional power available to stabilize each interferometer, we used a dedicated ADuC7020 for each PLL. The feedback signal (FS) used by the PLL is a portion of the output of the photo-detector monitoring the same interferometer the PLL is controlling. An ADC channel, preceded by a low-pass filter with a bandwidth of 1 KHz, is used to acquire this signal. The intensity of this signal can be related to the relative phase φ between the cores that are involved in the 2-path interferometer:

$$FS(\varphi) = \frac{M - m}{2} \cos(\varphi) + \frac{M + m}{2}, \quad (1)$$

where M and m are the maximum and the minimum, respectively, of the interference fringes. In order to actively control this phase, a fiber-based phase-shifter has been introduced in each arm of each interferometer, as shown in Figure 1. A DAC channel is used to control, via an high-voltage driver, the phase shifter. The firmware installed on the microcontroller can be divided into two main blocks: one generates a triangular ramp at the DAC output to uniformly scan the interferometer relative phase, the other contains the code that implements the digital PID used for the phase stabilization. Its behaviour is described in the flowchart in Figure 2.

The PID block is divided into three main stages. The starting point is a serial input from the user, that communicates to the microcontroller the locking phase, i.e., the phase where the interferometer should be locked. This command activates the first stage, where the voltage applied to the phase-shifter is scanned, in order to produce a phase variation slightly bigger than 2π . Meanwhile, the FS is measured by the microcontroller ADC to find the maximum (M) and the minimum (m) of the interference fringes. By knowing these two parameters, it is possible to invert Equation 1 to determine the value of the FS corresponding to the desired locking phase, called Locking Point (LP). The locking phase value, i.e. the LP, is a parameter which can be arbitrarily fixed by the user in

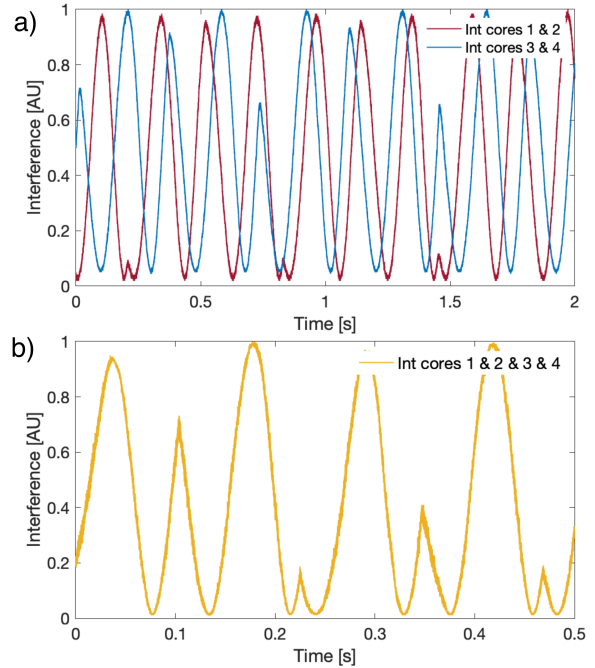


Figure 3: Visibility fringes of the interferometers. **a)** Interference signals as a function of time for the two independent interferometers between cores 1 & 2 and cores 3 & 4. Measured visibility of $V_{1\&2} = 0.981 \pm 0.008$ and $V_{3\&4} = 0.945 \pm 0.011$. **b)** Interference signal from the three interferometers. In this measurement, the first two independent interferometers are locked to a fixed position. Measured visibility of $V_{1\&2\&3\&4} = 0.989 \pm 0.004$.

the range from 0 to 2π . During the second stage, the same phase range is scanned in order to approach the locking point, with a precision determined by the user-defined threshold Th_A . By measuring the FS signal during this scan, it is also possible to select the slope of the interference fringe used for locking, which allows us to stabilize the relative phase over the all range $[0, 2\pi]$. As soon as $|FS - LP| < Th_A$, the PID loop [23] starts operating (stage 3). Otherwise, if this condition can not be reached, the algorithm restarts back from the first stage. Once activated, the PID loop keeps acting as long as the condition $|FS - LP| < Th_B$ remains verified. The Th_B threshold fixes the maximum tolerable difference between FS and the desired LP. If this condition is not verified, the PID loop stops and the algorithm starts back from the first stage, allowing for an automatic re-locking.

Results

In order to phase-stabilize the cores of the multicore fiber, we built the three interferometers as described in the previous paragraph. The first parameter to be evaluated in these interferometers is the visibility, which is directly linked to the performance of a quantum or

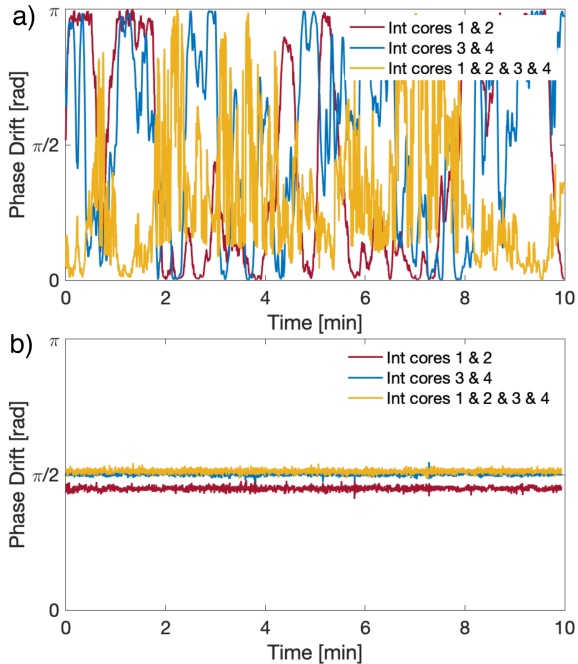


Figure 4: Phase drifts of the non stabilized and stabilized multicore interferometers over 10 minutes acquisition. a) Phase drift between two-cores and four-cores interferometers without active phase stabilization. b) Phase drift of a) but with active phase stabilization loops. Different colours represent the three different configurations (red and blue, two paths interferometers; yellow, four paths interferometer).

classical communication protocol, in terms of expected error rate. In Figure 3 on the preceding page), the red (blue) curve shows the interference fringes obtained by driving, with a triangular shape, the fiber phase-shifter in the 2-path interferometer involving cores 1 & 2 (3 & 4) of the MCF. These two interferometers, as shown in the experimental setup in Figure 1, are independent. We measured a visibility of $V_{1&2} = 0.981 \pm 0.008$ and $V_{3&4} = 0.945 \pm 0.011$. The third interferometer involves all of the four cores and, to evaluate its visibility, the two independent interferometers (involving cores 1 & 2 and cores 3 & 4 separately) must be locked to a specific phase, in order to balance the two powers entering in the third BS. Through the first two PLLs, we have locked the two independent interferometers to around 50% of the fringe and, exploiting the third phase shifter, we generated a triangular ramp in the overall interferometer, as shown in Figure 3b) with yellow color. The visibility value we measured is $V_{1&2&3&4} = 0.989 \pm 0.004$.

Subsequently to the visibility measurement, we investigated the possibility of stabilizing the four different cores of the MCF for a certain amount of time. The stabilization of the relative phase between the cores of a multicore fiber is an essential property for the reliable transmission of the quantum states, both in quantum

key distribution applications but also in more advanced quantum network protocols. We report in Figure 4a) the temporal drift of the relative phases between the cores, observed with the unlocked interferometers over a continuous and free-running acquisition of ten minutes. Figure 4b) shows the same acquisition in which we have turned on the three automatic PLL systems, to actively compensate the drifts. In order to stabilize all the different cores, we have first locked the two independent interferometers involving cores 1 & 2 and cores 3 & 4, and subsequently we have locked the overall interferometer. To be noted that, in case of fast and abrupt drifts in the fiber, i.e. when the locking position is suddenly lost, our phase lock loop system is able to automatically re-lock to the same position, by restarting the PLL algorithm from the first stage (see Figure 2). Another important point to be highlighted is that the polarization of the different cores was stable over 100 minutes of acquisition time.

In addition, we further investigated the free-running acquisition in order to better characterize the signal phase fluctuations in the multicore fiber, for different fiber lengths. To this end, we made additional 30-minutes acquisitions, with 6 Hz sampling rate, of the cores interference signals for multiple strands. In Figure 5 we show the results of these measurements. In the left panel, we report the power spectrum of the interference signal as a function of frequency for one of the two-cores interferometers (1 & 2). In the right panel we report the same measurement for the four-cores interferometer.

Discussion

Optical interferometers are the basic component for optical signal processing. More specifically, fiber-based interferometers are widely used for different applications, spanning from sensing, and optical communication to quantum physics and gravitational wave detections. Multipaths interferometers are used for manipulating quantum states and high-dimensional unitary operations, and in this work we demonstrated the possibility of stabilizing a long-distance multicore fiber through a simple and scalable setup. For example, we might imagine to use a wavelength multiplexing approach for transmitting quantum and classical light in the same fiber. One of these channels could be used for stabilizing the drift of the relative phase as demonstrated in [19] In the same direction, we have also demonstrated that the phase drift is not directly related to the length of the multicore fiber. In fact, by looking at Figure 5, both configurations seem quite insensitive to the overall interferometric size. This behaviour can be explained by considering that most of the phase fluctuations comes from the fibers connecting the rack-mount optical patch panel to the rest of

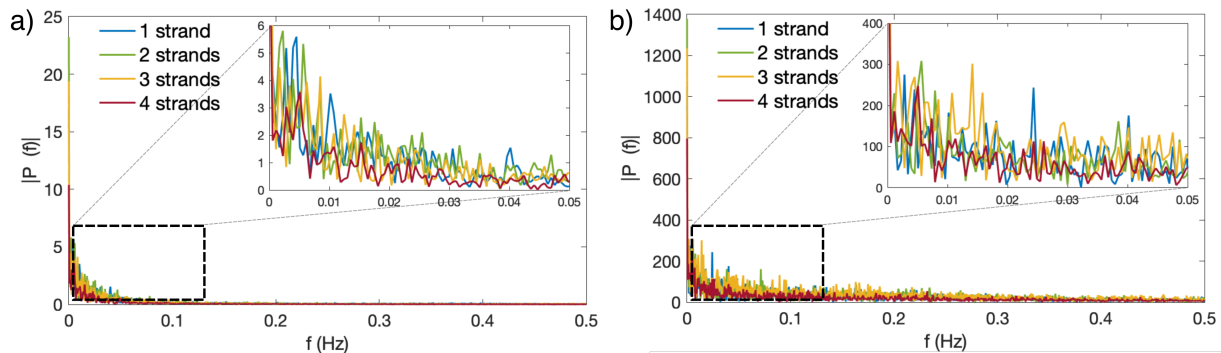


Figure 5: Frequency analysis of the interference signals. a) Two-cores interferometers for the four different strands. b) Four-cores interferometer for the four different strands. Different colours represent different strands. Each measurement has been acquired for 30 minutes of non-locked system.

the experimental setup, located on a table as close to it as possible. In other words, we can assume that the most unstable portion of the interferometric apparatus is the fan-in and fan-out part [24].

The second evidence, from Figure 5b), is that the 4-cores interferometer is more sensitive to phase fluctuations than the 2-path configurations. In fact, the spectral density function of the 4-cores interferometer is about 2 order of magnitudes higher as compared to the 2-paths one. This fact, as already demonstrated in [25–29], could be quite useful for sensing applications, both classical and quantum.

To be noted that in our demonstration, we have used cascaded interferometers for analysing independently all the optical signals, but new devices have been recently introduced for multi-port beam splitter [30]. These devices are properly designed for acting as interfaces between single-mode fibers and multicore fibers, and could increase the overall stability of the system.

Summarizing, we here presented a scalable and efficient method for stabilizing the phase drifts in multicore fiber. The presented method can in principle be applied to longer fiber distances and larger core counts, by using the same technology. Our demonstration paves the way towards future investigations and applications of multicore fibers in quantum communication.

Acknowledgements

Funding

This work is supported by the Center of Excellence, SPOC - Silicon Photonics for Optical Communications (ref DNR123), by the EraNET Cofund Initiatives QuantERA within the European Union’s Horizon 2020 research and innovation program grant agreement No.731473 (project SQUARE), by the NATO Science for Peace and Security program under grant G5485, by the Italian Government through Project INCIPIC

and Project PRIN 2017 FIRST, and from the European Union through OpenQKD-project MuQuAKE (project number: 857156).

References

- [1] K. Saitoh and S. Matsuo, “Multicore fiber technology,” *Journal of Lightwave Technology*, vol. 34, no. 1, pp. 55–66, 2016.
- [2] Y. Amma, Y. Sasaki, K. Takenaga, S. Matsuo, J. Tu, K. Saitoh, M. Koshihara, T. Morioka, and Y. Miyamoto, “High-density multicore fiber with heterogeneous core arrangement,” in *2015 Optical Fiber Communications Conference and Exhibition (OFC)*, pp. 1–3, IEEE, 2015.
- [3] H. Hu, F. Da Ros, M. Pu, F. Ye, K. Ingerslev, E. P. da Silva, M. Nooruzzaman, Y. Amma, Y. Sasaki, T. Mizuno, *et al.*, “Single-source chip-based frequency comb enabling extreme parallel data transmission,” *Nature Photonics*, vol. 12, no. 8, pp. 469–473, 2018.
- [4] T. Hayashi, T. Nagashima, T. Nakanishi, T. Morishima, R. Kawawada, A. Mecozzi, and C. Antonelli, “Field-deployed multi-core fiber testbed,” in *2019 24th OptoElectronics and Communications Conference (OECC) and 2019 International Conference on Photonics in Switching and Computing (PSC)*, pp. 1–3, IEEE, 2019.
- [5] T. Hayashi, T. Taru, O. Shimakawa, T. Sasaki, and E. Sasaoka, “Low-crosstalk and low-loss multi-core fiber utilizing fiber bend,” in *Optical Fiber Communication Conference*, p. OWJ3, Optical Society of America, 2011.
- [6] T. Hayashi, Y. Tamura, T. Hasegawa, and T. Taru, “Record-low spatial mode dispersion and ultra-low loss coupled multi-core fiber for ultra-long-haul transmission,” *Journal of Lightwave Technology*, vol. 35, no. 3, pp. 450–457, 2017.

- [7] . I.-T. S. W. Q. meeting, “Standardization of optical fibre cable and components for sdm technology,” 2020.
- [8] H. Yuan, M. Furdek, A. Muhammad, A. Saljoghei, L. Wosinska, and G. Zervas, “Space-division multiplexing in data center networks: on multi-core fiber solutions and crosstalk-suppressed resource allocation,” *Journal of Optical Communications and Networking*, vol. 10, no. 4, pp. 272–288, 2018.
- [9] M. Nooruzzaman and T. Morioka, “Multi-core fibers in submarine networks for high-capacity undersea transmission systems,” in *2017 Optical Fiber Communications Conference and Exhibition (OFC)*, pp. 1–3, IEEE, 2017.
- [10] J. Dynes, S. Kindness, S.-B. Tam, A. Plews, A. Sharpe, M. Lucamarini, B. Fröhlich, Z. Yuan, R. Penty, and A. Shields, “Quantum key distribution over multicore fiber,” *Optics express*, vol. 24, no. 8, pp. 8081–8087, 2016.
- [11] D. Bacco, B. Da Lio, D. Cozzolino, F. Da Ros, X. Guo, Y. Ding, Y. Sasaki, K. Aikawa, S. Miki, H. Terai, *et al.*, “Boosting the secret key rate in a shared quantum and classical fibre communication system,” *Communications Physics*, vol. 2, no. 1, pp. 1–8, 2019.
- [12] B. Da Lio, D. Bacco, D. Cozzolino, F. Da Ros, X. Guo, Y. Ding, Y. Sasaki, K. Aikawa, S. Miki, H. Terai, *et al.*, “Record-high secret key rate for joint classical and quantum transmission over a 37-core fiber,” in *2018 IEEE photonics conference (IPC)*, pp. 1–2, IEEE, 2018.
- [13] Y. Ding, D. Bacco, K. Dalgaard, X. Cai, X. Zhou, K. Rottwitt, and L. K. Oxenløwe, “High-dimensional quantum key distribution based on multicore fiber using silicon photonic integrated circuits,” *npj Quantum Information*, vol. 3, no. 1, p. 25, 2017.
- [14] G. Cañas, N. Vera, J. Cariñe, P. González, J. Cardenas, P. Connolly, A. Przysieszna, E. Gómez, M. Figueroa, G. Vallone, *et al.*, “High-dimensional decoy-state quantum key distribution over multicore telecommunication fibers,” *Physical Review A*, vol. 96, no. 2, p. 022317, 2017.
- [15] D. Bacco, Y. Ding, K. Dalgaard, K. Rottwitt, and L. K. Oxenløwe, “Space division multiplexing chip-to-chip quantum key distribution,” *Scientific reports*, vol. 7, no. 1, pp. 1–7, 2017.
- [16] G. B. Xavier and G. Lima, “Quantum information processing with space-division multiplexing optical fibres,” *Communications Physics*, vol. 3, no. 1, pp. 1–11, 2020.
- [17] B. Da Lio, D. Bacco, D. Cozzolino, N. Biagi, T. N. Arge, E. Larsen, K. Rottwitt, Y. Ding, A. Zavatta, and L. K. Oxenløwe, “Stable transmission of high-dimensional quantum states over a 2-km multicore fiber,” *IEEE Journal of Selected Topics in Quantum Electronics*, vol. 26, no. 4, pp. 1–8, 2019.
- [18] D. Cozzolino, B. Da Lio, D. Bacco, and L. K. Oxenløwe, “High-dimensional quantum communication: Benefits, progress, and future challenges,” *Advanced Quantum Technologies*, p. 1900038, 2019.
- [19] B. Da Lio, D. Cozzolino, B. Nicola, Y. Ding, K. Rottwitt, A. Zavatta, D. Bacco, and L. K. Oxenløwe, “Path-encoded high-dimensional quantum communication over a 2 km multicore fiber,” *arXiv:2103.05992*, 2021.
- [20] A. Alarcón, J. Argillander, G. Lima, and G. B. Xavier, “Few-mode fibre technology fine-tunes losses of quantum communication systems,” 2021.
- [21] R. S. Luís, B. J. Puttnam, G. Rademacher, A. Marotta, C. Antonelli, F. Graziosi, A. Mecozzi, T. Hayashi, T. Nakanishi, S. Shinada, Y. Awaji, H. Furukawa, and N. Wada, “Evaluation of dynamic skew on spooled and deployed multicore fibers using o-band signals,” in *Optical Fiber Communication Conference (OFC) 2020*, p. T4J.4, Optical Society of America, 2020.
- [22] B. J. Puttnam, R. S. Luis, G. Rademacher, A. Marotta, C. Antonelli, A. Mecozzi, F. Graziosi, T. Hayashi, T. Nakanishi, Y. Awaji, H. Furukawa, and N. Wada, “Dynamic skew measurements in a deployed 4-core fiber,” in *Conference on Lasers and Electro-Optics*, p. STu4R.1, Optical Society of America, 2020.
- [23] L. Rozsa, “Design and implementation of practical digital pid controllers,” *IFAC Proceedings Volumes*, vol. 22, no. 18, pp. 115–121, 1989.
- [24] X.-M. Hu, W.-B. Xing, B.-H. Liu, D.-Y. He, H. Cao, Y. Guo, C. Zhang, H. Zhang, Y.-F. Huang, C.-F. Li, and G.-C. Guo, “Efficient distribution of high-dimensional entanglement through 11 km fiber,” *Optica*, vol. 7, pp. 738–743, Jul 2020.
- [25] Z. Zhao, Z. Liu, M. Tang, S. Fu, L. Wang, N. Guo, C. Jin, H.-Y. Tam, and C. Lu, “Robust in-fiber spatial interferometer using multicore fiber for vibration detection,” *Optics express*, vol. 26, no. 23, pp. 29629–29637, 2018.
- [26] G. M. D’Ariano and M. G. Paris, “Arbitrary precision in multipath interferometry,” *Physical Review A*, vol. 55, no. 3, p. 2267, 1997.
- [27] L. Gan, R. Wang, D. Liu, L. Duan, S. Liu, S. Fu, B. Li, Z. Feng, H. Wei, W. Tong, *et al.*, “Spatial-division multiplexed mach-zehnder interferometers in heterogeneous multicore fiber for multiparameter measurement,” *IEEE Photonics Journal*, vol. 8, no. 1, pp. 1–8, 2016.
- [28] K. U. Schreiber and J.-P. R. Wells, “Invited review article: Large ring lasers for rotation sensing,”

Review of Scientific Instruments, vol. 84, no. 4, p. 041101, 2013.

- [29] G. Weihs, M. Reck, H. Weinfurter, and A. Zeilinger, “All-fiber three-path mach-zehnder interferometer,” *Optics letters*, vol. 21, no. 4, pp. 302–304, 1996.
- [30] L. Pereira, A. Rojas, G. Cañas, G. Lima, A. Delgado, and A. Cabello, “Universal multi-port interferometers with minimal optical depth,” *arXiv preprint arXiv:2002.01371*, 2020.